Heliyon 9 (2023) e21282

Contents lists available at ScienceDirect

Heliyon

journal homepage: www.cell.com/heliyon

Xanthohumol alleviates palmitate-induced inflammation and prevents osteoarthritis progression by attenuating mitochondria dysfunction/NLRP3 inflammasome axis

Weichao Sun [a,b,1], Jiaji Yue [a,1], Tianhao Xu [c,d], Yinxing Cui [a,f], Dixi Huang [a,f], Houyin Shi [e], Jianyi Xiong [a], Wei Sun [a,**], Qian Yi [f,d,*]

[a] Department of Orthopedics, Shenzhen Second People's Hospital (The First Affiliated Hospital of Shenzhen University), Shenzhen, Guangdong, 518035, China
[b] The Central Laboratory, Shenzhen Second People's Hospital (The First Affiliated Hospital of Shenzhen University), Shenzhen, Guangdong 518035, China
[c] Department of Anesthesiology, The Affiliated Hospital of Southwest Medical University, Luzhou, Sichuan Province, 646000, China
[d] Laboratory of Anesthesia and Organ Protection, Southwest Medical University, Luzhou, Sichuan, 646099, China
[e] Department of Orthopedics, The Affiliated Traditional Chinese Medicine Hospital of Southwest Medical University, China
[f] Department of Physiology, School of Basic Medical Science, Southwest Medical University, Luzhou, Sichuan, 646000, China

ARTICLE INFO

Keywords:
Osteoarthritis
Palmitate
Xanthohumol
Mitochondria dysfunction
NLRP3 inflammasome
AMPK/NF-κB signaling pathway

ABSTRACT

Osteoarthritis (OA) is a prevalent chronic degenerative joint disease worldwide. Obesity has been linked to OA, and increased free fatty acid levels (e.g., palmitate) contribute to inflammatory responses and cartilage degradation. Xanthohumol (Xn), a bioactive prenylated chalcone, was shown to exhibit antioxidative, anti-inflammatory, and anti-obesity capacities in multiple diseases. However, a clear description of the preventive effects of Xn on obesity-associated OA is unavailable. This study aimed to assess the chondroprotective function of Xn on obesity-related OA. The *in vitro* levels of inflammatory and ECM matrix markers in human chondrocytes were assessed after the chondrocytes were treated with PA and Xn. Additionally, *in vivo* cartilage degeneration was assessed following oral administration of HFD and Xn. This study found that Xn treatment completely reduces the inflammation and extracellular matrix degradation caused by PA. The proposed mechanism involves AMPK signaling pathway activation by Xn, which increases mitochondrial biogenesis, attenuates mitochondrial dysfunction, and inhibits NLRP3 inflammasome and the NF-κB signaling pathway induced by PA. In summary, this study highlights that Xn could decrease inflammation reactions and the degradation of the cartilage matrix induced by PA by inhibiting the NLRP3 inflammasome and attenuating mitochondria dysfunction in human chondrocytes.

* Corresponding author. Department of Physiology, School of Basic Medical Science, Southwest Medical University, Luzhou, Sichuan, 646000, China.
** Corresponding author. Department of Orthopaedics, Shenzhen Second People's Hospital (The First Affiliated Hospital of Shenzhen University), 3002 Sungang West Road, Futian, Shenzhen, Guangdong, 518035, China.
E-mail addresses: 414464705@qq.com (W. Sun), yiqian@swmu.edu.cn (Q. Yi).
[1] Equal contribution.

https://doi.org/10.1016/j.heliyon.2023.e21282
Received 28 April 2023; Received in revised form 16 October 2023; Accepted 18 October 2023

1. Introduction

With a prevalence of approximately 28 % in the global population over 60 years, osteoarthritis (OA) stands among some of the most prevalent joint diseases. Characteristic features of OA include inflammation, cartilage degeneration, pain, and physical disability [1,2]. Epidemiological analysis suggests that the incidence of OA is associated with numerous risk factors, including previous joint damage, aging, gender, genetic factors, joint anatomical factors, and obesity [3,4]. Currently, pain management and end-stage joint replacement surgery are the most preferred strategies for OA treatment [3,5]. However, the occurrence of postoperative adverse outcomes and the finite lifespan of the prosthesis present a major obstacle to current therapies. Therefore, contemporary research has shifted its focus to pathogenesis and developing new strategies for the prevention of early OA.

Obesity is a major risk factor leading to the onset and progression of OA; it not only increases the burden on weight-bearing joints like the knee and the hip but also affects lipid metabolism. Elevations in the levels of free fatty acids (FFAs), such as stearic acid (SA) and palmitate (PA), are linked to obesity [6,7]. These FFAs are important proinflammatory factors. Studies have reported that FFAs are key contributors to endothelial dysfunction, insulin resistance, cardiac dysfunction, and ischemic cardiomyopathy [8–10]. The excessive accumulation of these FFAs may lead to the initiation of inflammatory signaling pathways (e.g., toll-like receptors), eventually causing cell dysfunction [11]. Studies have further demonstrated that elevated FFA levels in cartilage tissues, synovial fluid, and synovium of patients with OA are associated with disease severity [7,12,13]. These results indicate the relationship between obesity and OA. However, a comprehensive elucidation of its underlying mechanisms is currently unavailable.

Xanthohumol (Xn), a prenylated chalcone, is a primary bioactive component extracted from *Humulus lupulus* L (the hop plant). Xn was previously shown to possess anti-tumor, anti-inflammatory, anti-obesity, and anti-oxidative properties. Kenta et al. reported that Xn suppresses the angiogenesis of pancreatic cancer by blocking the NF-κB signaling [14]. Moreover, Xn can inhibit the NF-κB signaling pathway and protect against LPS-induced acute lung injury [15]. Additionally, Xn could suppress hepatic steatosis, expression of pro-inflammatory genes, and non-alcoholic fatty liver in the WTD-induced obesity model [16]. Xn has also been reported to prevent age-related brain damage and hepatic alterations by eliminating age-related oxidation stress and inflammation [17,18]. However, the involvement of Xn in OA, another obesity-related and inflammatory disease, is not yet explained. We attempted to understand the anti-inflammatory, chondroprotective, and mitochondria-protective properties of Xn in palmitate-induced chondrocytes in this study, which would help explore a potential novel pharmacological agent for OA treatment.

2. Materials and methods

2.1. Reagents and chemicals

Endotoxin-free Xn was purchased from Aladdin and CCK-8 from Beyotime Institute of Biotechnology. The Gress reagent nitrite measurement kit was commercially procured from Cell Signaling Technology. Human PGE2 ELISA kits were purchased from Solarbio Science & Technology [19]. Penicillin/streptomycin and Fetal bovine serum were purchased from Gbico. Nutrient Mixture F12 (DMEM/F12), and Dulbecco's modified Eagle's medium was supplied by Hyclone.

2.2. Preparation and culture of human primary chondrocytes

The Ethics Review Committee at the Shenzhen Second People's Hospital granted its approval for the collection of cartilage tissues from patients. After each patient received a thorough explanation of the investigation and provided written informed consent (Ethic no.20211215005-FS01), samples were collected for this study. Tissues from the human articular cartilage were collected from volunteer donors who had undergone joint replacement or joint surgery. The samples were washed thrice with PBS containing penicillin and streptomycin and then cut into small fragments (1–3 mm^3). The minced samples were placed in 1 mg/mL collagenase II (Sigma) at 37 °C for 16 h in a shaker; digestion was performed multiple times until collagen was completely dissolved. After digestion, the suspension was filtered with a 100 mm nylon cell strainer to remove matrix debris, and the cells were then collected after centrifugation at a rate of 1000 rpm for 10 min [20]. Cells were resuspended thoroughly and subcultured in chondrocyte growth medium (DMEM/F12, 10 % FBS, 100 μg/mL streptomycin, and 100 IU/mL penicillin) using a CO_2 (5 %) incubator at 37 °C. The medium was replaced as the cells attached and passaged when they reached 80 % confluence. Chondrocytes from only passage 1 (P1) and passage 2 (P2) were included in the experiments. Chondrocyte morphology was studied using toluidine blue staining [21].

2.3. CCK-8 assay

Human primary chondrocytes were seeded on 96-well cell culture plates at a density of 1×10^4 cells/well, which were subjected to overnight incubation. The Xn concentration range used in the assay was determined based on previous studies. After incubation with Xn for 48 h, the viability of cells was measured using a cell counting kit-8 as per the standard procedures. Briefly, the culture medium and CCK-8 solution were mixed at a ratio of 10:1, following which 100 μL of the mixture was introduced into each of the wells. Afterward, it was incubated for 1 h at 37 °C in an incubator, and its absorbance at 450 nm was recorded via a microplate reader [22].

2.4. Griess reaction and PGE2 ELISA

IL-1β (10 ng/mL) treatment of the cells with and without Xn was done for 24h to measure the levels of NO and PGE2. The culture

medium was first harvested, and then the Gress reagent nitrite measurement kit (Cell Signaling Technology) and human PGE2 ELISA kit (Solarbio Science & Technology) were used to quantify the NO and PGE2 levels, respectively, as laid out in the instruction handbook of the kit [23]. All the assays were repeated at least thrice.

2.5. Real-time PCR

As per the instructions provided by the manufacturer, total RNA was isolated from the human articular chondrocytes using TRIzol reagent (Invitrogen). Afterward, cDNA synthesis was done using 1 μg of total RNA with the aid of the PrimeScript™ RT Reagent Kit and gDNA Eraser (Takara). Quantitative RT-PCR was conducted with SYBR Green Supermix (BioRad) using aViiA7™ Real-Time PCR System (Applied Biosystems) [20]. Each experiment was done at least thrice, and all samples were normalized to *GAPDH* as the standard. Table 1 contains a list of the primer sequences designed for this study.

2.6. Western blots

Whole protein extraction from chondrocytes was done using lysis buffer (50 mM Tris-Hcl, 150 mM NaCl, pH 7.4, and 0.1 % SDS) with protease inhibitor supplement. The nuclear and cytoplasmic proteins from the chondrocytes were extracted using a nuclear and cytoplasmic protein extraction kit. Cells were lysed for 30 min with lysis buffer on ice by swirling each 10 min. The protein solution was then centrifuged for 10 min at a rate of 15,000g at 4 °C. Using a BCA protein assay kit (Pierce), the samples' protein concentration was determined [24].

The denatured protein solution was exposed to SDS-PAGE (12 %) and then transferred onto a PVDF membrane. Membrane blocking was carried out with 5 % non-fat dry milk (1 h at room temperature), which was incubated at 4 °C with primary antibodies for an entire night. As the membrane underwent three washes with TBST, the secondary antibodies were applied, and the mixture was incubated at room temperature for an hour. Using an ECL reagent (ThermoFisher), bands on the membrane were developed, and analysis of immunoreactive bands was performed using the ImageJ software [25]. All the results were repeated at least thrice. Primary antibodies specifically directed against GAPDH (1:1000), COX-2 (1:1000), iNOS (1:1000), MMP1 (1:5000), MMP3 (1:5000), MMP13 (1:1000), PGC-1α (1:1000), TFAM (1:1000), AMPKα (1:1000), and p-AMPKα (1:1000) were purchased from Proteintech. ADAMTS5 (1:500) was purchased from ABclonal, and collagen II (1:500) was purchased from ThermoFisher Scientific; Human Reactive Inflammasome Antibody Sampler Kit II, p-IκBα (1:1000), IκBα (1:1000), p65 (1:1000), p-p65 (1:1000), anti-rabbit IgG, HRP-linked Antibody (1:1000), anti-mouse IgG, and HRP-linked Antibody (1:1000) were purchased from Cell Signaling Technology.

2.7. Immunofluorescence

Seeding of the chondrocytes was done in 24-well glass plates at a fixed density of 1×10^4 cells per well. Cell treatment was done with 10 ng/mL PA in the absence and presence of Xn for 24h for collagen II and MMP13 stain, and for 2h in case of p65 stain. The glass-seeded chondrocyte monolayers were fixed with 4 % paraformaldehyde (room temperature, 15 min) after they were washed thrice with PBS. Following another PBS wash, 0.3 % Triton X-100 (in PBS) was introduced to permeabilize the cells (10 min at room temperature). The cells were then blocked using 5 % BSA for 30 min. Chondrocytes were incubated with collagen II, MMP13, and p65 primary antibodies overnight at 4 °C. The cells were then washed thrice with PBS and incubated with Alexa Fluor® 647-conjugated goat anti-rabbit IgG (1:500) for 1h in the darkness at room temperature. Finally, the cells were incubated with DAPI for nuclei staining. Under a fluorescence microscope, the images were captured [20].

Table 1
Primers for RT-PCR used in this study.

Gene	Forward primer	Reverse primer
IL-1β	5′-TACGAATCTCCGACCACCA-3′	5′-GGACCAGACATCACCAAGC-3′
TNF-α	5′-GTCAGATCATCTTCTCGAACC-3′	5′-CAGATAGATGGGCTCATACC-3′
iNOS	5′-GACGAGACGGATAGGCAGAG-3′	5′-CACATGCAAGGAAGGGAACT-3′
COX-2	5′-GAGAGATGTATCCTCCCACAGTCA-3′	5′-GACCAGGCACCAGACCAAAG-3′
MMP1	5′-CTGTTCAGGGACAGAATGTGC-3′	5′-TTGGACTCACACCATGTGTT-3′
MMP3	5′-TGCGTGGCAGTTTGCTCAGCC-3′	5′-GAATGTGAGTGGAGTCACCTC-3′
MMP13	5′-GGCTCCGAGAAATGCAGTCTTTCTT-3′	5′-ATCAAATGGGTAGAAG TCGCCATGC-3′
Adamts5	5′-GGTCAAGGTCCCATGTGCAAC-3′	5′-GAATGCGGCCATCTTGTCATC-3′
Collage II	5′-CTGTCCTTCGGTGTCAGGG-3′	5′-CGGCTTCCACACATCCTTAT-3′
NLRP3	5′-CGTGAGTCCCATTAAGATGGAGT-3′	5′-CCCGACAGTGGATATAGAACAGA-3′
ASC	5′-GCGCTGGAGAACCTGACCGC-3′	5′-CTCCTGCAGGCCCATGTCGC-3′
Caspase-1	5′-GAAAGCCCACATAGAGAAGG-3′	5′-CTCTTTCAGTGGTGGGCATC-3′
PGC-1α	5′-AGCCTCTTTGCCCAGATCTT-3′	5′-GGCAATCCGTCTTCATCCAC-3′
TFAM	5′-CCAAAAAGACCTCGTTCAGCTT-3′	5′-CTTCAGCTTTTCCTGCGGTG-3′
D-loop	5′-CTATCACCCTATTAACCACTCA-3′	5′-TTCGCCTGTAATATTGAACGTA-3′
18sRNA	5′-TAGAGGGACAAGTGGCGTTC-3′	5′-CGCTGAGCCAGTCAGTGT-3′
GAPDH	5′-GGAGCGAGATCCCTCCAAAAT-3′	5′-GGCTGTTGTCATACTTCTCATGG-3′

2.8. Molecular docking

The structure of AMPK (PDB ID: 4CFF) was retrieved from the RCSB Protein Data Bank (https://www.rcsb.org/) and used as the receptor for molecular docking. The 3D structure of Xn was obtained from the PubChem website (https://pubchem.ncbi.nlm.nih.gov/) and used as a ligand for molecular docking (PubChem ID: 639,665). Molecular docking between small ligand molecules and the receptor protein was performed using the AutoDockTools1.5.7 software. PYMOL 2.5.2 was used to analyze the flexibility of ligand binding to the pocket residues [26].

2.9. ATP assay

The level of ATP in chondrocytes was measured using an ATP assay kit from the Beyotime Institute of Biotechnology following the guidelines of the manufacturer [27]. Briefly, the treated cells were subjected to lysis and centrifugation at 12000*g* (4 °C) for 5min. Afterward, 20 μl of the collected supernatant was added to 100 μl working solution in a 96-well plate. The luminescence was detected using a microplate reader.

2.10. Reactive oxygen species (ROS) assay

Using a ROS assay kit (Beyotime Institute of Biotechnology Inc.) [28], ROS was detected by the fluorescent probe 2′, 7′–dichlorofluorescein diacetate (DCFHDA). Briefly, cells were separated by centrifugation, stained with DCFHDA, and then examined using a microplate reader after 30 min of incubation in the darkness at 37 °C.

2.11. Lipid peroxidation malondialdehyde (MDA) assay

A lipid peroxidation MDA assay kit helped in the detection of lipid peroxidation levels. Thiobarbituric acid (TBA) and MDA can interact in an acidic environment at high temperatures to generate the red MDA-$(TBA)_2$ adduct. Briefly, cells were collected and centrifuged for 15 min at 12000g. The supernatant obtained was treated with TBA and the reaction product was determined by spectrophotometry at 535 nm [29].

2.12. Animal models

Sprague-Dawley (SD) male wild-type (WT) rats (8 weeks old) were procured from the Cloud-Clone Corp., Wuhan. Rats were housed in a sterile setting (temperature = 27 °C) with a 12h light-dark cycle and 50 % humidity. The Committee for Animal Use and Care at Southwest Medical University approved all animal protocols and procedures involved in this study (Ethic no. 20211124-043). A high-fat diet (HFD) was applied to the rats for six weeks before the construction of an OA model, which was built on the instability of the medial meniscus (DMM) caused by surgical therapy, as was already mentioned [30]. Briefly, 40 mg/kg of 2 % (w/v) pentobarbital was administered intraperitoneally to the rats to make them unconscious. Microsurgical scissors were used to cut the medial meniscus tibial ligament, and the medial patellar tendon was used to open the right knee joint capsule. However, in a sham control group, the medial meniscus tibial ligament was not cut. In the present investigation, rats were classified into three groups at random: the OA group (DMM), the OA group receiving XN treatment (DMM + XN), and the sham control group (sham).

2.13. Histopathological analysis

The knee joint's calcification was removed with a 10 % EDTA solution after it had been fixed with 4 % paraformaldehyde (24 h, 4 °C). To create frontal serial slices with a thickness of 5 m, the tissue was dehydrated, cleared, embedded in paraffin blocks, and sliced. Afterward, safranin O-fast green (S–O) staining was done for the slides, and a light microscope was used to identify the degree of cartilage degeneration [20].

2.14. Immunohistochemical assay

MMP3 and collagen II expression levels were detected in the cartilage by immunohistochemistry. Briefly, the slides were dewaxed, rehydrated, and sealed with 5 % BSA for 30 min after a 20-min incubation with 0.4 % pepsin (Sangon Biotech Co., Ltd.) in 5 mM HCl to repair the antigen. Then, in the presence of primary antibodies specific to MMP3 (1:500) and collagen II (1:50) overnight (at 4 °C), incubation of the slides was done. After 50 min (room temperature) of incubation, the slides were subjected to incubation with HRP-conjugated goat anti-rabbit (1:50), and images were captured with an Olympus BX51 microscope (Olympus Corporation) [20].

2.15. Statistical analysis

All experiments were repeated at least thrice. The data were presented as mean ± SD. The software called GraphPad Prism version 8.0 was used for statistical analysis. A Student t-test with two-tailed and unpaired samples was used to make a comparison between the two groups. Multiple groups were compared using a single-factor analysis of variance (ANOVA) and a posttest (Bonferroni). In addition, $P < 0.05$ indicated the significance level.

3. Results

3.1. Cytotoxicity of Xn on human chondrocytes

The molecular chemical structure of Xn is presented in Fig. 1A. The toluidine blue staining of proteoglycan revealed the spindle-shaped morphology of human primordial chondrocytes (Fig. 1B). The expression levels of collage II, MMP13, and MMP3 in normal human and OA chondrocytes were examined. The results showed that in comparison to OA chondrocytes, normal chondrocytes expressed more collage II and less MMP3 and MMP13 (Fig. 1C). Additionally, only human chondrocytes in passages 1 and 2 were used in the next experiments. Our findings demonstrated that small quantities of Xn had no considerable cytotoxic effect on human chondrocytes. However, following treatment with a concentration of 20 μM, the vitality of chondrocytes was considerably decreased (Fig. 1D and E). Therefore, an Xn concentration of 10 μM was used in subsequent experiments.

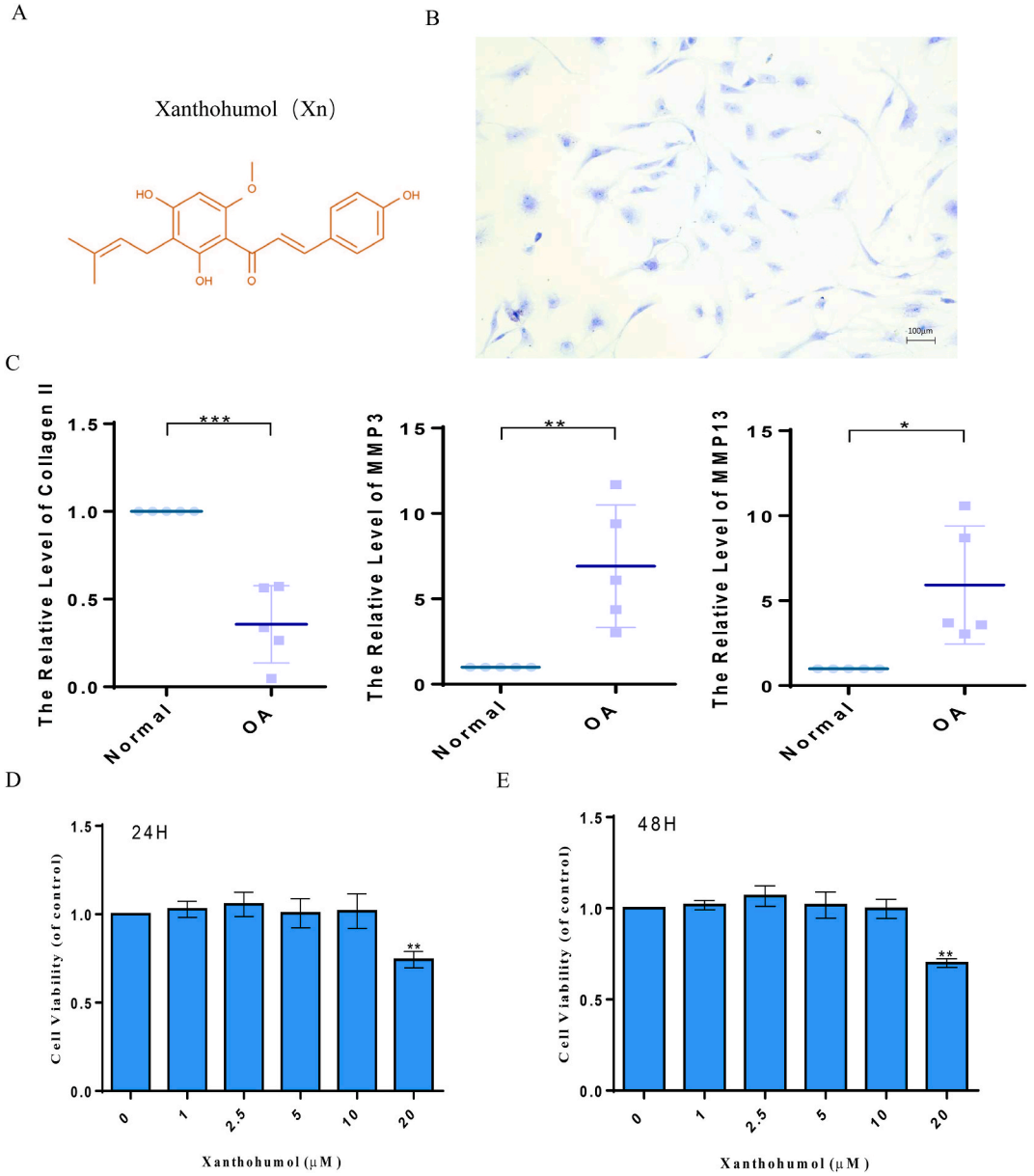

Fig. 1. The cytotoxicity of Xn on human chondrocytes. A. Chemical structure of Xn. B. Human primary chondrocytes examined by toluidine blue staining. C. Expression of collagen II, MMP3, and MMP13 detected by qPCR in normal human and OA chondrocytes. D and E. Cytotoxic effects of Xn on human chondrocytes determined at 24h and 48h by CCK8 assay. *P < 0.05, **P < 0.01, and ***P < 0.001.

3.2. PA-induced inflammatory mediators in human chondrocytes are blocked by Xn

Herein, qPCR, western blotting, and ELISA were conducted to evaluate the expression and production of IL-1, TNF-, iNOS, COX-2, NO, and PGE2, thus examining the effects of Xn on PA-induced inflammation of chondrocytes. Xn suppressed the IL-1β expression, and TNF-α was stimulated by PA (Fig. 2A–B). Additionally, the outcomes demonstrate that Xn suppressed COX-2 and iNOS expression that was induced by PA at the protein and gene levels (Fig. 2C–E). The ELISA results suggested that Xn inhibited PA-induced NO and PGE2 production (Fig. 2D). Thus, it can be proposed that Xn inhibited the expression and production of PA-induced inflammatory mediators in human chondrocytes.

3.3. Xn attenuates PA-induced ECM degradation in human chondrocytes

The effects of Xn on collagen II, MMP1, MMP3, MMP13, and Adamts5 were investigated by qPCR, western blotting, and immunofluorescence to ascertain the effects of Xn on the synthesis of ECM and its degradation induced by PA. According to the observations, Xn enhanced the collagen II mRNA expression in response to PA stimulation while inhibiting the expression of MMP1, MMP3, MMP13, and Adamts5 mRNAs (Fig. 3A). Following PA stimulation, Xn (10 μM) elevated the protein level of collagen II while inhibiting the protein levels of MMP1, MMP3, MMP13, and Adamts5 (Fig. 3B–C). Additionally, collagen II and MMP13 immunofluorescence staining revealed that following PA stimulation, Xn stimulated collagen II expressions and inhibited MMP13 expression (Fig. 3D). Our results suggest that Xn attenuates PA-induced ECM degradation by inhibiting collagen II synthesis and the synthesis of ECM-degrading enzymes in human chondrocytes.

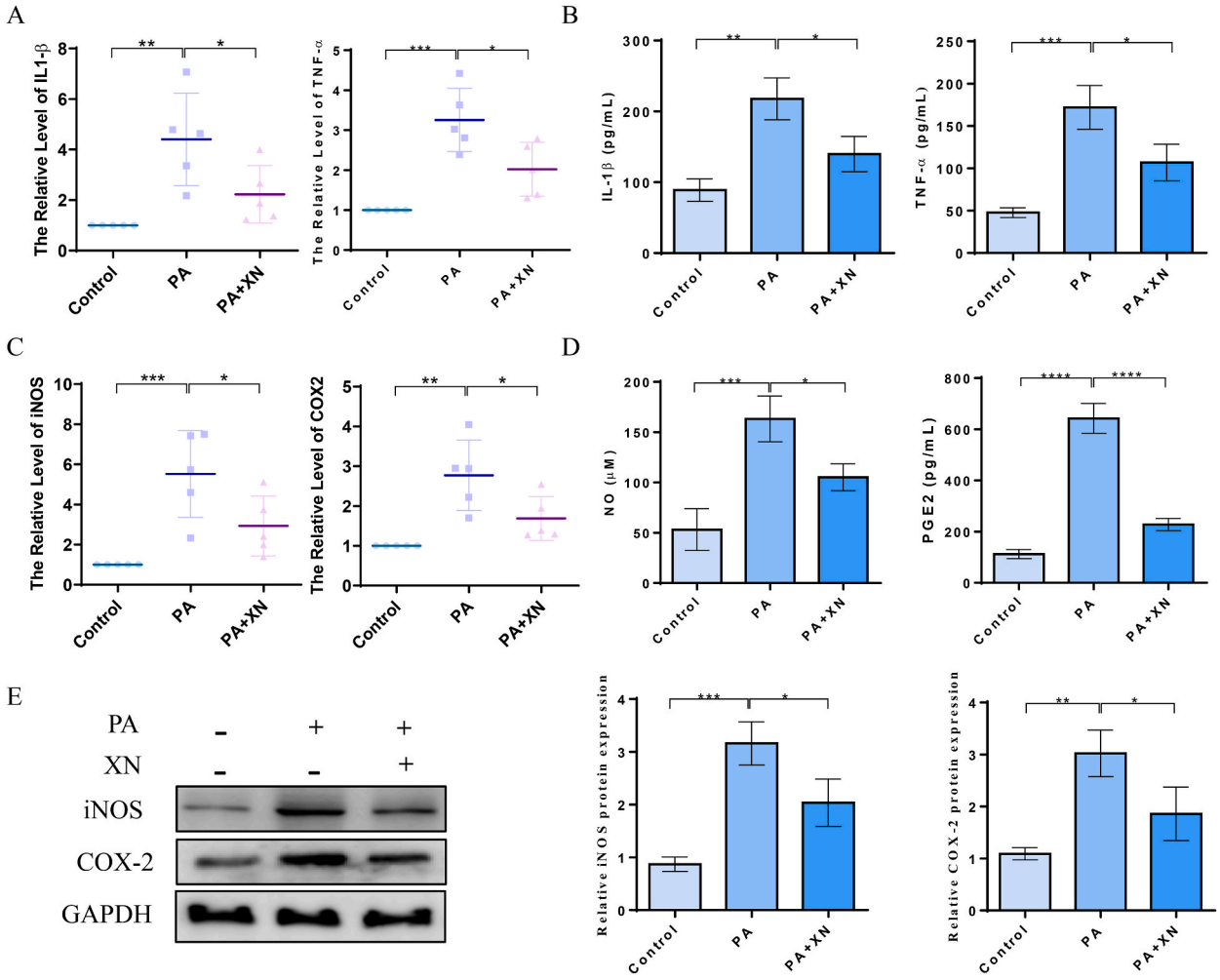

Fig. 2. Blocking the levels of PA-induced inflammatory mediators by Xn in human chondrocytes. A. mRNA expression of IL-1β and TNF-α detected using qPCR. B. Production of IL-1β and TNF-α detected using ELISA. C. mRNA expression of iNOS and COX-2 detected using qPCR. D. Production of NO and PGE2 detected using ELISA. E. Protein expression of COX2 and iNOS detected using western blotting and quantified. *P < 0.05, **P < 0.01, and ***P < 0.001.

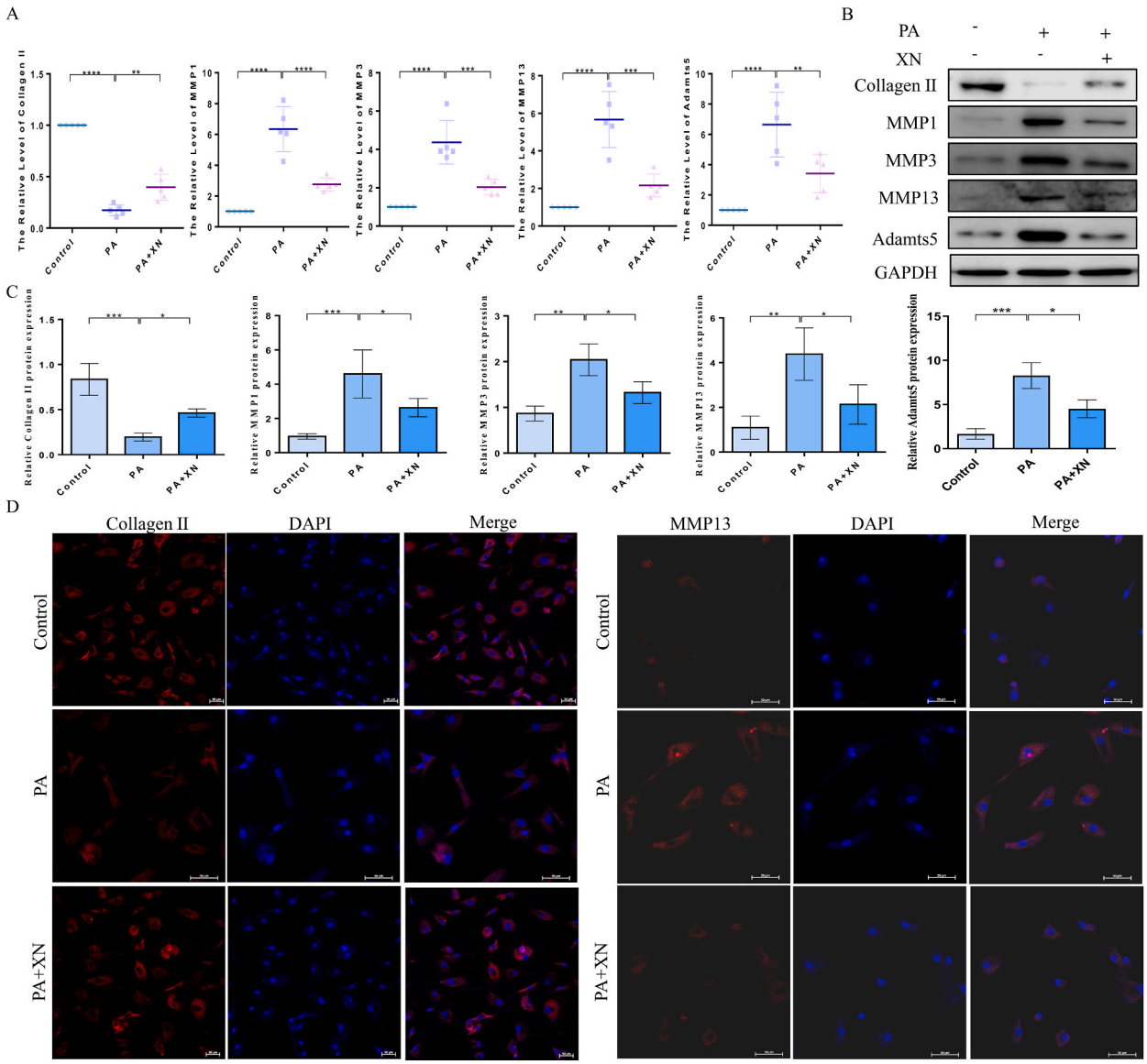

Fig. 3. Attenuation of PA-induced ECM degradation by Xn in human chondrocytes. A. mRNA expression of collagen II, MMP1, MMP3, MMP13, and Adamts5 detected using qPCR. Protein expression of collagen II, MMP1, MMP3, MMP13, and Adamts5 detected using western blotting (B) and quantification results (C). D. Expression of collagen II and MMP13 detected by immunofluorescence. *P < 0.05, **P < 0.01, ***P < 0.001 and ****P < 0.0001.

3.4. Xn prevents PA-induced NF-κB activation in human chondrocytes

To ascertain the anti-inflammatory effects of Xn on PA-treated chondrocytes, the expression of p65, p-p65, IκBα, and p-IκBα was examined using immunofluorescence and western blotting. According to the observations, Xn pretreatment substantially attenuated the phosphorylation of p65, which was remarkably elevated by PA stimulation (Fig. 4A–B). In PA-induced chondrocytes, Xn pretreatment enhanced IκBα protein levels and lowered IκBα phosphorylation levels (Fig. 4A–B). Additionally, Xn pretreatment reduced p65 expression in the nucleus of PA-induced chondrocytes, according to the results of the immunofluorescence staining (Fig. 4C). Our findings indicated that Xn inhibited p65 translocation and IκBα degradation in human chondrocytes, thus preventing PA-induced NF-κB activation.

3.5. Xn inhibits PA-NLRP3 inflammasome axis-induced inflammation and ECM degradation

According to recent reports, palmitate, the most abundant among all saturated FFAs, serves as a secondary signal for the NLRP3

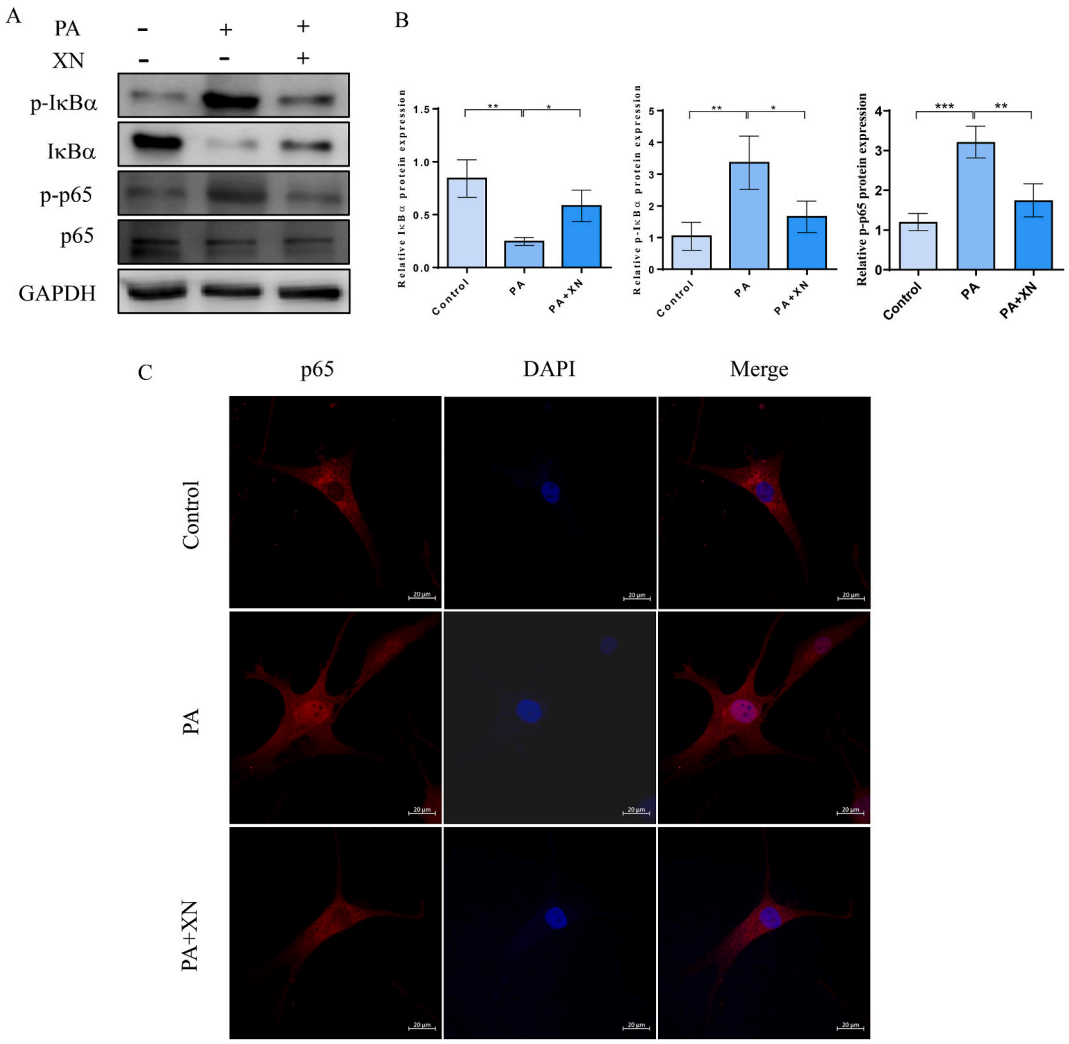

Fig. 4. Prevention of PA-induced NF-κB activation by Xn in human chondrocytes. Protein expression of p-IkBα, IkBα, p-p65, and p65 detected using western blotting (A) and quantified (B). C. Nuclear translocation of p65 observed by immunofluorescence. *P < 0.05, **P < 0.01, and ***P < 0.001.

inflammasome to become active. NLRP3 was involved in the maturation and release of IL-1β, which played a significant role in OA progression. Therefore, the effects of Xn on PA-induced activation of NLRP3 inflammasome were investigated. Our results suggested that PA stimulation considerably increased the mRNA levels of NLRP3, ASC, and caspase 1, while Xn pretreatment considerably prevented these increases (Fig. 5A). Western blotting revealed that Xn pretreatment reduced the expression of NLRP3, ASC, caspase-1, pro-caspase-1, IL-1β, and pro-IL-1β in chondrocytes that were stimulated by PA (Fig. 5B–C). Thus, our findings suggest that Xn may have inhibited PA from inducing IL-1β production via the mechanism of preventing the activation of the NLRP3 inflammasome in human chondrocytes.

3.6. Xn promotes mitochondrial biogenesis and prevents mitochondrial dysfunction

Mitochondrial dysfunction contributes to the inflammatory response by activating the NLRP3 inflammasomes. Moreover, Xn has been shown to activate the AMPK signaling pathway which plays a significant function in maintaining mitochondrial homeostasis. Therefore, the effects of Xn on mitochondrial biogenesis were investigated. Our studies revealed that PA-induced downregulation of p-AMPKα, PGC-1α, and TFAM expression was suppressed by Xn (Fig. 6A–C). To confirm whether the effects of Xn on PA-induced inflammation and ECM degradation are mediated by AMPK activation, compound C was used. The level of p-AMPKα, TFAM and collagen II in PA-treated chondrocytes incubated with Xn in the presence of compound C were significantly decreased, and the level of expression of NLRP3 and MMP3 was increased (Fig. 6D). Computational molecular docking analysis between Xn and AMPK was performed by AutoDock 4. The structures of Xn and AMPK were obtained and analyzed (Fig. 6E and F). The results showed that Xn formed hydrogen bonds with AMPK residues ARG78 and GLN81 (Fig. 6G). Moreover, PA-induced ROS accumulation and MDA

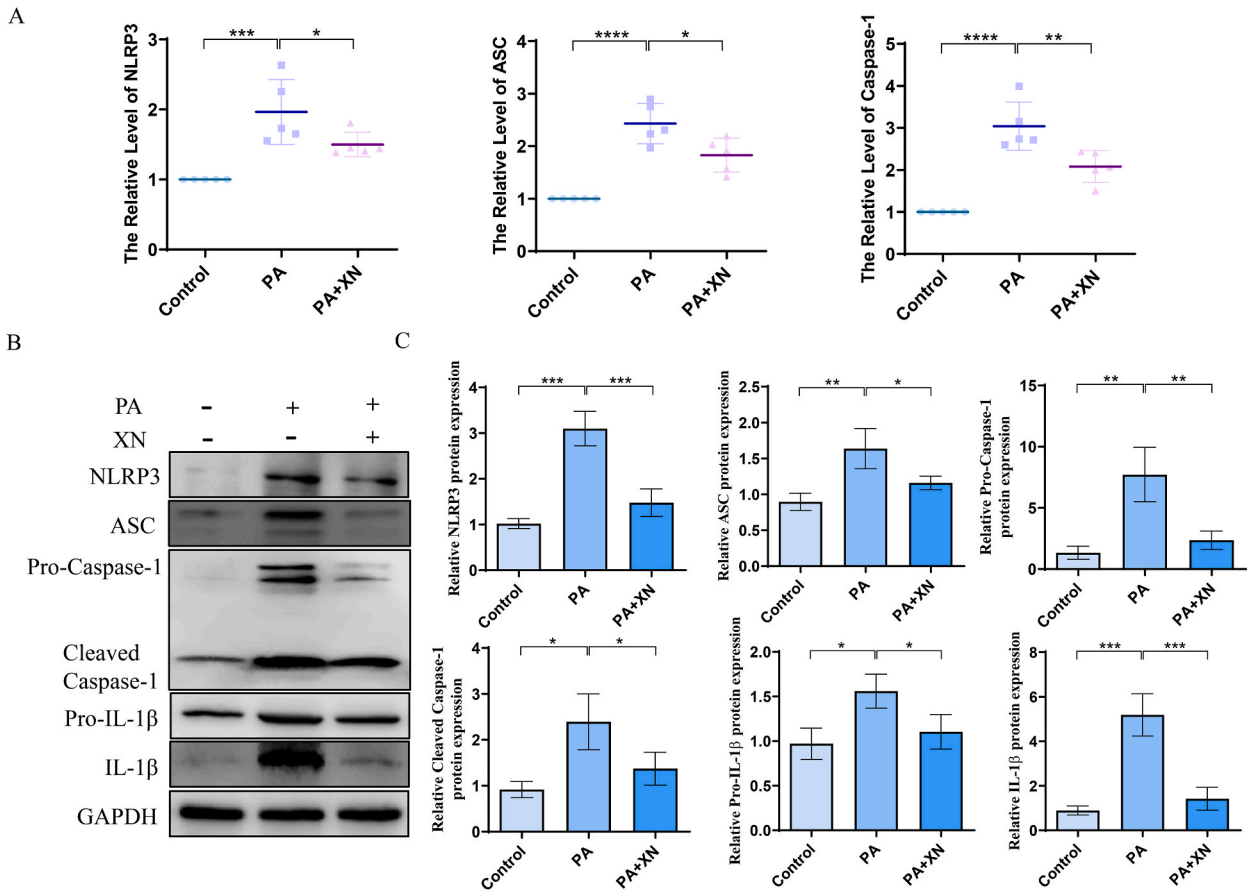

Fig. 5. Inhibition of PA-NLRP3 inflammasome axis-induced inflammation and ECM degradation by Xn. A. mRNA expression of NLRP3, ASC, and caspase 1 detected using qPCR. Protein expression of NLRP3, ASC, caspase-1, pro-caspase-1, IL-1β, and pro-IL-1β detected using western blotting (B) and quantification results (C). *P < 0.05, **P < 0.01, ***P < 0.001 and ****P < 0.0001.

elevation were also inhibited by Xn (Fig. 6H–I). Furthermore, Xn increased the expression of ATP and mtDNA, which were down-regulated by PA (Fig. 6J–K). Therefore, our data provide proof that Xn may increase mitochondrial biogenesis and prevent PA-induced mitochondrial dysfunction as well as NLRP3 inflammasome activation.

3.7. Xn alleviates OA progression in the DMM rat model

A rat OA model was constructed, which then administered with Xn (20 mg/kg/2 days) intraperitoneally to evaluate the effect of Xn on OA progression *in vivo*. S–O staining revealed that the DMM group's articular cartilage had remarkably less articular cartilage than that in the sham control group, which had a red-dyed, normal, and smooth surface (Fig. 7A). The red-dyed region thickened, and the articular cartilage surface was smoother in the Xn-treated group compared to those the DMM group (Fig. 7A), suggesting that Xn may have played a role in attenuating the degradation of the cartilage matrix. MMP3 and collagen II immunohistochemistry were also observed in the OA model. The MMP3 expression level was remarkably higher in the DMM group than in the sham group, whereas it was lower in the DMM + CAPE group (Fig. 7B). The collagen II expression level was remarkably lower in the DMM group than in the sham group, whereas it was higher in the DMM + CAPE group (Fig. 7B).

4. Discussion

OA is among the most prevalent inflammatory disorders with complex pathogenesis. It presents multiple symptoms such as chronic joint pain, inflammation, and joint cartilage damage. Obesity and obesity-associated metabolic factors are considered to be key factors in promoting OA [31,32]. Aberrant accumulation of adipose tissue, which increases the mechanical stress on joints, is a primary contributor to obesity-related OA. However, individuals with obesity have a higher probability of developing OA in small joints of the body [33]. Irregular lipid metabolism and numerous adipocytokines are thought to have a significant contribution to the initiation and pathogenesis of OA [34,35]. Previous studies demonstrate that the FFA levels are quite high in the synovial fluid and the cartilage of patients with OA, which has the potential to trigger chronic inflammation in the chondrocytes [31,36]. For example, PA the most

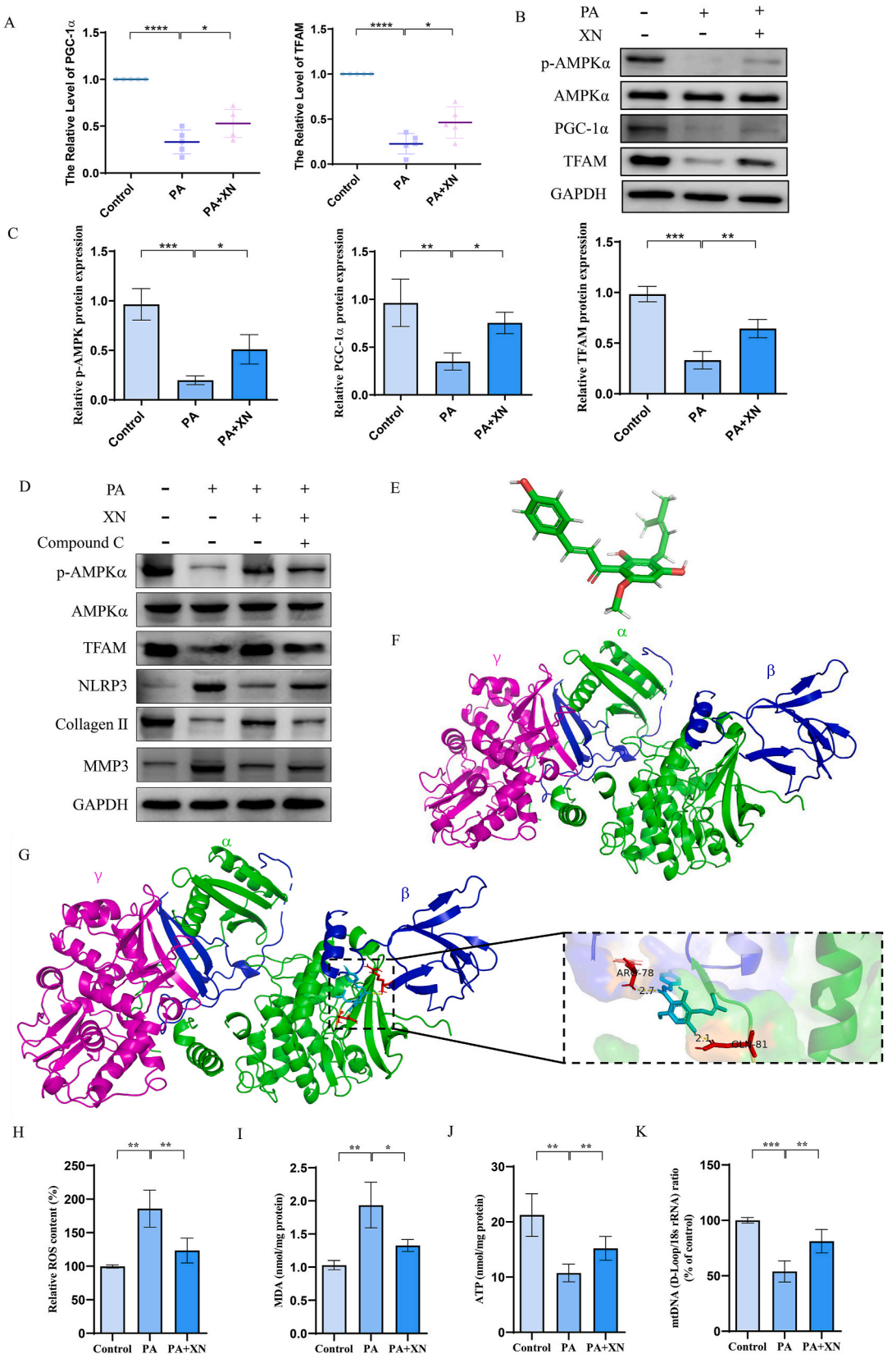

(caption on next page)

Fig. 6. Increased mitochondrial biogenesis and prevention of mitochondrial dysfunction by Xn. A. mRNA expression of PGC-1α and TFAM detected using qPCR. Protein expression of p-AMPKα, AMPKα, PGC-1α, and TFAM detected using western blotting (B) and quantification results (C). D. Protein expression of p-AMPKα, AMPKα, TFAM, NLRP3, Collagen II, and MMP3 detected using western blotting with or without compound C treatment. E. Modular structure of Xn. F. The modular structure of AMPK. G. Interaction between Xn and AMPK. H. Content of ROS measured by a detection kit. I. Content of MDA measured by a detection kit. J. Content of ATP measured by detection kit. K. Expression of mtDNA detected using qPCR. *P < 0.05, **P < 0.01, ***P < 0.001 and ****P < 0.0001.

common saturated fatty acid found in the human body [37], was reported to induce expression of the inflammatory mediator IL-6, thus promoting ECM degradation in the chondrocytes [38]. And growing evidence shown that PA was used to study high-fat diet (HFD) related diseases. Such as, PA-treated HK-2 renal tubular cells were used for *in vitro* assessments of obesity-induced nephropathy [39]. The *in vitro* model of non-alcoholic fatty liver disease was established by treating HepG2 cells with PA [40]. Moreover, PA-induced osteoarthritis cell models was well used to study obesity-related OA [41,42], hence, we used PA treated chondrocyte cell model for further studies. Increasing evidence has shown that natural compounds possess chondroprotective properties; as they can repress inflammatory responses, they could be potential agents in treating OA [43,44]. Only limited strategies are available for treating obesity-related OA. Oral administration of resveratrol could alleviate high-fat diet-induced osteoarthritis pathology in mice [45] indicating the potential of natural compounds in preventing obesity-related OA. Herein, Xn, a prenylated chalcone, can inhibit inflammatory responses, and ECM degradation caused by PA in human chondrocytes. In the present study, we have illustrated its underlying mechanism and its chondroprotective function in rats have been elucidated.

According to the findings from the present study, PA was a potent inducer of inflammation in chondrocytes, consistent with a previous study [38]. We detected enhanced expression of iNOS, IL-1β, COX-2, TNF-α, MMP-1, 3 and 13, and Adamts5, and decreased collagen II expression in PA-treated human chondrocytes. All of these are active markers for inflammatory response and ECM degradation in OA. Additionally, increased synthesis of NO and PGE2 increased the production of iNOS, COX-2, IL-1β, and TNF-α in PA-treated human chondrocytes, which was inhibited by Xn. Moreover, Xn significantly suppressed MMP1, MMP3, MMP13, and Adamts5 synthesis and reduced the deterioration rate of collagen II in PA-treated chondrocytes. These outcomes suggest that Xn could alleviate PA-induced inflammatory response and ECM degradation occurring in human chondrocytes, implying that Xn has tremendous potential in the treatment of obesity-related OA.

The possible mechanisms of Xn involved in the inhibition of PA-induced NLRP3 inflammasome activation were further investigated. NF-κB not only enhances the transcription of catabolic genes, like the family of MMPs and ADAMTSs, but also activates the expression of essential inflammation factors in OA chondrocytes, including COX2, iNOS, and PGE2, indicating the crucial function of this transcription factor in OA pathogenesis [46]. Our results revealed that Xn pretreatment inhibited p65 translocation to the nucleus from the cytoplasm in PA-induced chondrocytes. Moreover, the PA-induced NF-κB signaling stimulation was suppressed by Xn. These findings are in line with prior reports by Kenta and Lv, which described how Xn suppresses the angiogenesis of pancreatic cancer [14] and protects from acute lung injury induced by LPS [15] by inhibiting the NF-κB signaling pathway. Hence, the molecular mechanism involved in the inhibition of PA-induced OA by Xn might be linked to the NF-κB signaling pathway.

Although the NLRP3 inflammasome is essential in several human diseases, its function in OA pathogenesis remains unclear. Activated NLRP3 inflammasome can trigger caspase-1 that enhances the maturation and release of IL-1β. It is a crucial proinflammatory cytokine that links obesity to cellular dysfunction [47,48] and a mediator in the progression of OA [49,50]. it was recently discovered that PA has been involved in the activation of NLRP3 inflammasome in bone marrow-derived macrophages (BMMs) of obesity models [9]. The present study confirmed that PA could also activate the NLRP3 inflammasome in human chondrocytes. Thus, whether Xn could inhibit the NLRP3 inflammasome induced by PA was investigated. According to our findings, PA-induced overexpression of ASC, NLRP3, pro-caspase-1, caspase-1, pro- IL-1β, and IL-1β is inhibited via pretreatment of chondrocytes with Xn (Fig. 5). Thus, Xn may inhibit PA-induced IL-1β expression and OA progression by suppressing the NLRP3 inflammasome activation in human chondrocytes.

As previously established, the NLRP3 inflammasome can be activated by multiple danger signals, including ROS, nitric oxide (NO), and Ca^{2+} [51]. Excessive ROS generation led to ROS accumulation, which was identified as the most important activator of mitochondrial dysfunction [52]. Studies have shown that mitochondrial dysfunction contributes to several inflammatory disorders like neuro, heart, and kidney diseases by activating the NLRP3 inflammasomes [53,54]. Therefore, targeted inhibition of mitochondrial dysfunction may be a promising approach to attenuate the inflammatory reaction caused by the NLRP3 inflammasomes. For example, Fucoxanthin inhibits mitochondrial dysfunction and NLRP3 inflammasome in an AMPKα dependent manner [55]. The AMPKα/PGC-1α axis played a crucial role in maintaining mitochondrial homeostasis and in preventing mitochondrial dysfunction [56–58]. Janaiya reported that the anti-obesity effects of Xn relied on the initiation of the AMPKα signaling pathway [59]. In the present study, whether Xn could inhibit PA-induced mitochondrial dysfunction and NLRP3 inflammasomes by activating the AMPK signaling pathway was investigated. Xn revised the PA-induced downregulation of phosphorylated AMPKα, PGC-1α, and TFAM and inhibited PA-induced upregulation of ROS and MDA. In summary, Xn might constrain the stimulation of the NLRP3 inflammasome induced by PA in chondrocytes, which acts via increasing mitochondrial homeostasis and preventing mitochondrial dysfunction.

In this study, Xn attenuated the inflammatory response and ameliorated PA-induced degradation of ECM in chondrocytes through the activation of AMPKα/PGC-1α signaling pathway as well as inhibition of the NLRP3 inflammasome and the NF-κB signaling pathway (Fig. 7C). Additionally, in the DMM OA model, Xn could mitigate OA progression, in consistence with the *in vitro* experiments. Thus, Xn can act as an effective drug for OA treatment.

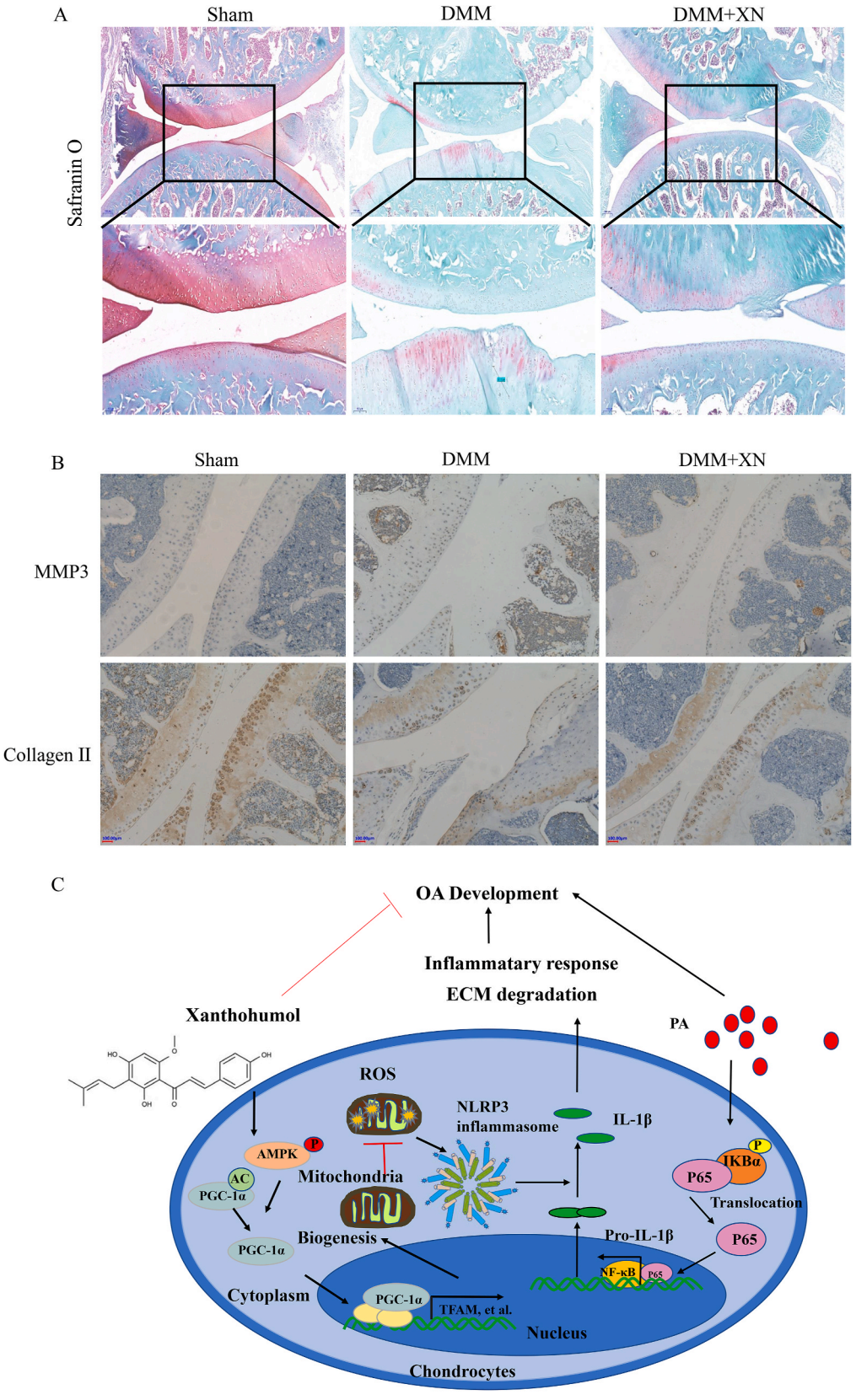

(caption on next page)

Fig. 7. Alleviation of OA progression by Xn in the DMM rat model. A. Degeneration of articular cartilage observed in S–O staining. B. Immunohistochemistry of MMP3 and collagen II employed to assess the effect of Xn on the cartilage in the DMM models. C. Schematic illustration of the prospective protection conferred by Xn and the underlying mechanism in PA-induced OA development.

Ethics statement

The Ethics Review Committee at the Shenzhen Second People's Hospital granted its approval for the collection of cartilage tissues from patients (Ethic no.20211215005-FS01). The Committee for Animal Use and Care at Southwest Medical University approved all animal protocols and procedures involved in this study (Ethic no. 20211124-043).

Data availability

No data were used to support this study.

Funding

This work was supported by funds from the Natural Sciences Foundation of China (No.82003126), Shenzhen Science and Technology Projects (No. JCYJ20190807102601647 and No. JCYJ20210324103604013), Sichuan Science and Technology Program (No.2022YFS0609 and No. 2022NSFSC1368), Luzhou Science and Technology Program (No. 2021-JYJ-71), Scientific Research Foundation of Southwest Medical University (No. 2021ZKMS009), and National Undergraduate Training Programs for Innovation and Entrepreneurship (No.202210632041).

CRediT authorship contribution statement

Jiaji Yue: Data curation. **Tianhao Xu:** Resources, Visualization. **Yinxing Cui:** Data curation. **Dixi Huang:** Data curation. **Houyin Shi:** Resources, Visualization. **Jianyi Xiong:** Supervision, Writing – review & editing. **Wei Sun:** Project administration, Supervision, Writing – review & editing. **Qian Yi:** Funding acquisition, Project administration, Supervision, Writing – original draft, Writing – review & editing.

Declaration of competing interest

The authors declare that they have no known competing financial interests or personal relationships that could have appeared to influence the work reported in this paper.

Acknowledgement

We thank Bullet Edits Limited for the linguistic editing and proofreading of the manuscript.

Appendix A. Supplementary data

Supplementary data to this article can be found online at https://doi.org/10.1016/j.heliyon.2023.e21282.

References

[1] J. Martel-Pelletier, et al., Osteoarthritis, Nat. Rev. Dis. Prim. 2 (2016), 16072.
[2] R.F. Loeser, et al., Osteoarthritis: a disease of the joint as an organ, Arthritis Rheum. 64 (6) (2012) 1697–1707.
[3] J.W. Bijlsma, F. Berenbaum, F.P. Lafeber, Osteoarthritis: an update with relevance for clinical practice, Lancet 377 (9783) (2011) 2115–2126.
[4] S. Glyn-Jones, et al., Osteoarthritis. Lancet 386 (9991) (2015) 376–387.
[5] A.J. Carr, et al., Knee replacement, Lancet 379 (9823) (2012) 1331–1340.
[6] G. Boden, Obesity and free fatty acids, Endocrinol Metab. Clin. N. Am. 37 (3) (2008) 635–646, viii-ix.
[7] X. Yu, et al., Asiatic acid ameliorates obesity-related osteoarthritis by inhibiting myeloid differentiation protein-2, Food Funct. 11 (6) (2020) 5513–5524.
[8] E. Fryk, et al., Hyperinsulinemia and insulin resistance in the obese may develop as part of a homeostatic response to elevated free fatty acids: a mechanistic case-control and a population-based cohort study, EBioMedicine 65 (2021), 103264.
[9] J.H. Xing, et al., NLRP3 inflammasome mediate palmitate-induced endothelial dysfunction, Life Sci. 239 (2019), 116882.
[10] X.M. Wei, et al., Plasma free fatty acid is associated with ischemic cardiomyopathy and cardiac dysfunction severity in systolic heart failure patients with diabetes, Chin Med J (Engl) 134 (4) (2020) 472–474.
[11] Y. Wang, et al., Saturated palmitic acid induces myocardial inflammatory injuries through direct binding to TLR4 accessory protein MD2, Nat. Commun. 8 (2017), 13997.
[12] K.W. Frommer, et al., Free fatty acids in bone pathophysiology of rheumatic diseases, Front. Immunol. 10 (2019) 2757.
[13] A. Van de Vyver, et al., Synovial fluid fatty acid profiles differ between osteoarthritis and healthy patients, Cartilage 11 (4) (2020) 473–478.
[14] K. Saito, et al., Xanthohumol inhibits angiogenesis by suppressing nuclear factor-kappaB activation in pancreatic cancer, Cancer Sci. 109 (1) (2018) 132–140.

[15] H. Lv, et al., Xanthohumol ameliorates lipopolysaccharide (LPS)-induced acute lung injury via induction of AMPK/GSK3beta-Nrf2 signal axis, Redox Biol. 12 (2017) 311–324.
[16] A. Mahli, et al., Therapeutic application of micellar solubilized xanthohumol in a western-type diet-induced mouse model of obesity, diabetes and non-alcoholic fatty liver disease, Cells 8 (4) (2019).
[17] L. Rancan, et al., Protective effect of xanthohumol against age-related brain damage, J. Nutr. Biochem. 49 (2017) 133–140.
[18] C. Fernandez-Garcia, et al., Xanthohumol exerts protective effects in liver alterations associated with aging, Eur. J. Nutr. 58 (2) (2019) 653–663.
[19] J. Fei, et al., Luteolin inhibits IL-1β-induced inflammation in rat chondrocytes and attenuates osteoarthritis progression in a rat model, Biomed. Pharmacother. 109 (2019) 1586–1592.
[20] W. Sun, et al., Caffeic acid phenethyl ester attenuates osteoarthritis progression by activating NRF2/HO-1 and inhibiting the NF-κB signaling pathway, Int. J. Mol. Med. 50 (5) (2022) 134.
[21] F. Liu, et al., Punicalagin attenuates osteoarthritis progression via regulating Foxo1/Prg4/HIF3α axis, Bone 152 (2021), 116070.
[22] D. Chen, et al., MSCs-laden silk Fibroin/GelMA hydrogels with incorporation of platelet-rich plasma for chondrogenic construct, Heliyon 9 (3) (2023), e14349.
[23] S. Wei, et al., Anti-inflammatory effects of Torin2 on lipopolysaccharide-treated RAW264.7 murine macrophages and potential mechanisms, Heliyon 8 (7) (2022), e09917.
[24] J. Feng, et al., hnRNP A1 promotes keratinocyte cell survival post UVB radiation through PI3K/Akt/mTOR pathway, Exp. Cell Res. 362 (2) (2018) 394–399.
[25] Y. Liao, et al., CIRP promotes the progression of non-small cell lung cancer through activation of Wnt/β-catenin signaling via CTNNB1, J. Exp. Clin. Cancer Res. 40 (1) (2021) 275.
[26] S.S. Wu, et al., Network pharmacology-based analysis on the effects and mechanism of the wang-Bi capsule for rheumatoid arthritis and osteoarthritis, ACS Omega 7 (9) (2022) 7825–7836.
[27] X. Mu, et al., An oligomeric semiconducting nanozyme with ultrafast electron transfers alleviates acute brain injury, Sci. Adv. 7 (46) (2021) eabk1210.
[28] H. Hao, et al., Farnesoid X receptor regulation of the NLRP3 inflammasome underlies cholestasis-associated sepsis, Cell Metabol. 25 (4) (2017) 856–867.e5.
[29] C. Wu, et al., A nonferrous ferroptosis-like strategy for antioxidant inhibition-synergized nanocatalytic tumor therapeutics, Sci. Adv. 7 (39) (2021) eabj8833.
[30] K. Warmink, et al., High-fat feeding primes the mouse knee joint to develop osteoarthritis and pathologic infrapatellar fat pad changes after surgically induced injury, Osteoarthritis Cartilage 28 (5) (2020) 593–602.
[31] J. Haywood, R.R. Yammani, Free fatty acid palmitate activates unfolded protein response pathway and promotes apoptosis in meniscus cells, Osteoarthritis Cartilage 24 (5) (2016) 942–945.
[32] T.M. Griffin, et al., Induction of osteoarthritis and metabolic inflammation by a very high-fat diet in mice: effects of short-term exercise, Arthritis Rheum. 64 (2) (2012) 443–453.
[33] T. Wang, C. He, Pro-inflammatory cytokines: the link between obesity and osteoarthritis, Cytokine Growth Factor Rev. 44 (2018) 38–50.
[34] C. Xie, Q. Chen, Adipokines: new therapeutic target for osteoarthritis? Curr. Rheumatol. Rep. 21 (12) (2019) 71.
[35] L. Chen, et al., Pathogenesis and clinical management of obesity-related knee osteoarthritis: impact of mechanical loading, J Orthop Translat 24 (2020) 66–75.
[36] K.W. Frommer, et al., Free fatty acids: potential proinflammatory mediators in rheumatic diseases, Ann. Rheum. Dis. 74 (1) (2015) 303–310.
[37] A.A. Raja, et al., Free fatty acid overload targets mitochondria: gene expression analysis of palmitic acid-treated endothelial cells, Genes 13 (10) (2022) 1704.
[38] O. Alvarez-Garcia, et al., Palmitate has proapoptotic and proinflammatory effects on articular cartilage and synergizes with interleukin-1, Arthritis Rheumatol. 66 (7) (2014) 1779–1788.
[39] C.C. Huang, et al., Empagliflozin ameliorates free fatty acid induced-lipotoxicity in renal proximal tubular cells via the PPARγ/CD36 pathway in obese mice, Int. J. Mol. Sci. 22 (22) (2021), 12408.
[40] Y. Ma, et al., Empagliflozin activates Sestrin2-mediated AMPK/mTOR pathway and ameliorates lipid accumulation in obesity-related nonalcoholic fatty liver disease, Front. Pharmacol. 13 (2022), 944886.
[41] X. Yu, et al., Asiatic acid ameliorates obesity-related osteoarthritis by inhibiting myeloid differentiation protein-2, Food Funct. 11 (6) (2020) 5513–5524.
[42] K.W. Frommer, et al., Free fatty acids in bone pathophysiology of rheumatic diseases, Front. Immunol. 10 (2019) 2757.
[43] P. Ma, et al., Chondroprotective and anti-inflammatory effects of amurensin H by regulating TLR4/Syk/NF-kappaB signals, J. Cell Mol. Med. 24 (2) (2020) 1958–1968.
[44] Y. Henrotin, A. Mobasheri, Natural products for promoting joint health and managing osteoarthritis, Curr. Rheumatol. Rep. 20 (11) (2018) 72.
[45] M. Jiang, et al., Oral administration of resveratrol alleviates osteoarthritis pathology in C57BL/6J mice model induced by a high-fat diet, Mediat. Inflamm. 2017 (2017), 7659023.
[46] M.C. Choi, et al., NF-kappaB signaling pathways in osteoarthritic cartilage destruction, Cells 8 (7) (2019).
[47] B. Bai, et al., NLRP3 inflammasome in endothelial dysfunction, Cell Death Dis. 11 (9) (2020) 776.
[48] B. Vandanmagsar, et al., The NLRP3 inflammasome instigates obesity-induced inflammation and insulin resistance, Nat. Med. 17 (2) (2011) 179–188.
[49] Z. Chen, et al., Inhibition of Nrf2/HO-1 signaling leads to increased activation of the NLRP3 inflammasome in osteoarthritis, Arthritis Res. Ther. 21 (1) (2019) 300.
[50] M.J. McAllister, et al., NLRP3 as a potentially novel biomarker for the management of osteoarthritis, Osteoarthritis Cartilage 26 (5) (2018) 612–619.
[51] Q. Liu, et al., The role of mitochondria in NLRP3 inflammasome activation, Mol. Immunol. 103 (2018) 115–124.
[52] M.Y. Wu, et al., The oxidative stress and mitochondrial dysfunction during the pathogenesis of diabetic retinopathy, Oxid. Med. Cell. Longev. 2018 (2018), 3420187.
[53] Z. Gong, et al., Mitochondrial dysfunction induces NLRP3 inflammasome activation during cerebral ischemia/reperfusion injury, J. Neuroinflammation 15 (1) (2018) 242.
[54] J.W. Yu, M.S. Lee, Mitochondria and the NLRP3 inflammasome: physiological and pathological relevance, Arch Pharm. Res. (Seoul) 39 (11) (2016) 1503–1518.
[55] S. Li, et al., Fucoxanthin alleviates palmitate-induced inflammation in RAW 264.7 cells through improving lipid metabolism and attenuating mitochondrial dysfunction, Food Funct. 11 (4) (2020) 3361–3370.
[56] R.C. Rabinovitch, et al., AMPK maintains cellular metabolic homeostasis through regulation of mitochondrial reactive oxygen species, Cell Rep. 21 (1) (2017) 1–9.
[57] M. Fontecha-Barriuso, et al., The role of PGC-1alpha and mitochondrial biogenesis in kidney diseases, Biomolecules 10 (2) (2020).
[58] Q. Zhang, et al., Quercetin attenuates diabetic peripheral neuropathy by correcting mitochondrial abnormality via activation of AMPK/PGC-1alpha pathway in vivo and in vitro, Front. Neurosci. 15 (2021), 636172.
[59] J.S. Samuels, R. Shashidharamurthy, S. Rayalam, Novel anti-obesity effects of beer hops compound xanthohumol: role of AMPK signaling pathway, Nutr. Metab. 15 (2018) 42.